Check for updates

Achieving solubility alteration with functionalized polydimethylsiloxane for improving the viscosity of supercritical CO_2 fracturing fluids†

Bin Liu, [ID] [a] Yanling Wang,*[a] Lei Liang[a] and Yijin Zeng*[b]

Supercritical carbon dioxide (SC-CO_2) fracturing technology has the characteristics of a large amount of fixed CO_2 and anhydrous fracturing. It has great application potential for developing unconventional oil and gas resources and mitigating the greenhouse effect. However, the low viscosity of SC-CO_2 limits the development of this technology. In this work, HS series thickeners were prepared *via* a ring-opening polymerization and hydrosilylation reaction by a molecular simulation-aided design method. The simulation results of cohesive energy density, interaction energy, and radial distribution function are consistent with the visualization experimental results, which proves that HS (hyperbranched siloxane) series thickeners have excellent solubility in SC-CO_2. HS-3 is the best thickener in the HS series. At 305.15 K and 10 MPa, 5 wt% HS-3 (60 s^{-1}) increases the viscosity of SC-CO_2 by 151 times, and the apparent viscosity is 3.024 mPa s. The apparent viscosity of SC-CO_2 was positively correlated with the pressure and concentration but negatively correlated with the temperature and shear rate. The results indicate that it is feasible to introduce an aliphatic group and polysiloxane into a SC-CO_2 thickener by hydrosilylation.

1. Introduction

The application of carbon dioxide has received extensive attention from scientists.[1] The two main reasons are as follows: (1) climatic changes caused by CO_2 cannot be overlooked, and (2) compared with hydrocarbon used as a raw material in the traditional industry, carbon dioxide can be economically beneficial and reduce environmental pollution.[2] CO_2 utilization was seen as a necessary cornerstone of successful large-scale carbon capture and storage.[3] Currently, 5% of the US annual crude oil production relies on CO_2-EOR (enhanced oil recovery) technology.[4] Under heterogeneous reservoir conditions, 1.1–3.3 barrels of crude oil can be produced for every ton of CO_2 injected.[5] The CO_2-EOR technology has the potential to be applied to 90% of the world's oilfields,[6] which means that 140 Gt CO_2 will be captured and fixed while enhancing the recovery rate.[3] In short, SC-CO_2 fracturing technology can improve the efficiency of shale gas development and reduce carbon emissions (Fig. 1).

At present, the core problem limiting this technology is that the viscosity is too low (0.02–0.05 mPa s) to carry the proppant

into the formation, and hence, it is necessary to study an excellent thickener. The reported SC-CO_2 thickener[7–9] containing fluorine has two disadvantages: (1) fluorinated monomers are too expensive to be widely used and (2) fluorine enters the biosphere *via* water circulation and cannot be metabolized by organisms.[10] The thickening mechanism of siloxane thickeners was reported:[11–15] (1) the formation of a Lewis acid hydrogen bond between a cosolvent and CO_2 and (2) the similar compatibility between the cosolvent and siloxane. The main characteristics of the reported hydrocarbon thickeners[16,17] are as follows: (1) low-molecular weight compounds have good solubility, but the thickening effect is poor and (2) under cosolvent conditions, long-chain polymer hydrocarbons are soluble in CO_2. Organosilicon thickeners often rely on cosolvents to improve the solubility, and cosolvent causes formation damage.[12] Silicone has the characteristics of low glass transition temperature, low binding energy, and good economy, which has great potential for the research and development of SC-CO_2
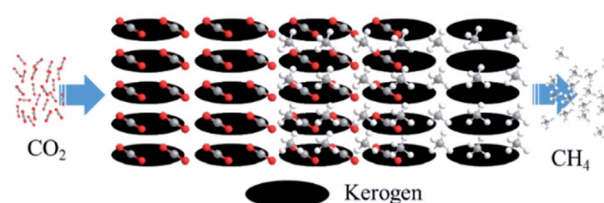
[a]School of Petroleum Engineering, China University of Petroleum (East China), Qingdao 266580, China. E-mail: wangyl@upc.edu.cn

[b]Sinopec Petroleum Exploration and Development Research Institute, Beijing, 10083, China. E-mail: zengyj.sripe@sinopec.com

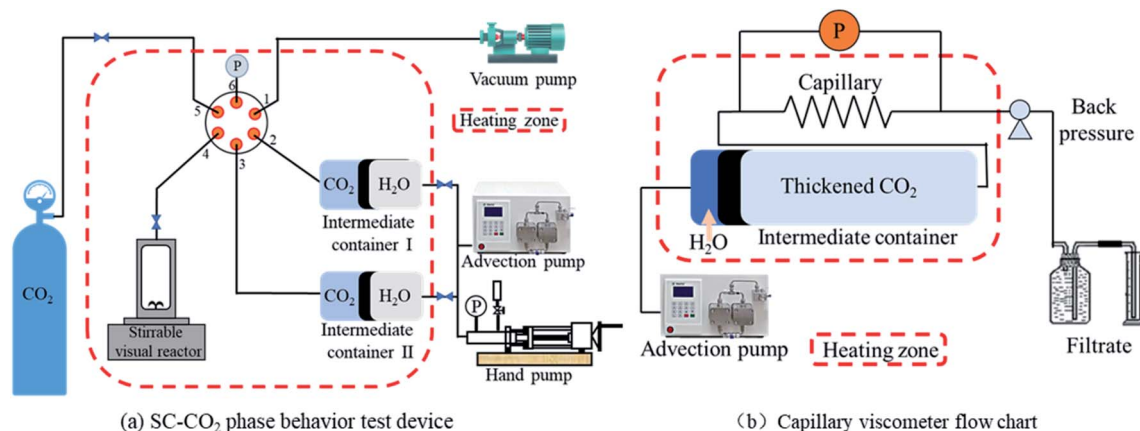† Electronic supplementary information (ESI) available. See DOI: 10.1039/d1ra02069b

Fig. 1 CO_2 and CH_4 competitive adsorption.

Fig. 2 (a) SC-CO$_2$ phase behavior test device. (b) Capillary viscometer flow chart.
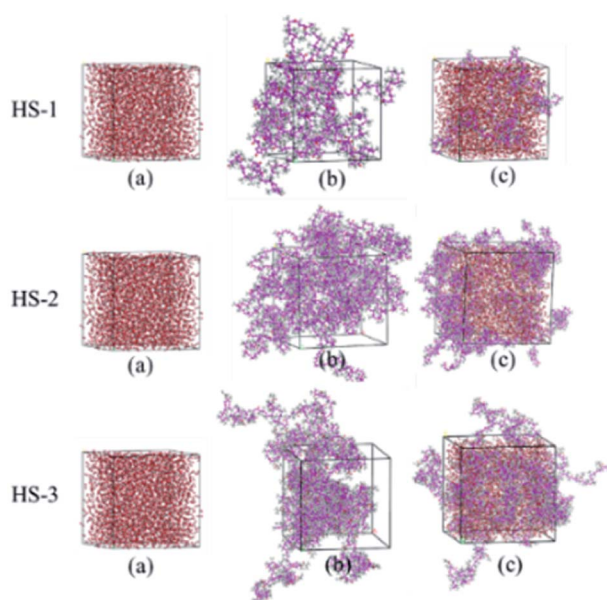

Fig. 3 Nine systems are built on the all-atom model: (a) CO$_2$ system composed of 2000 CO$_2$, (b) polymer system composed of 8 polymer chains, and (c) polymer–CO$_2$ system composed of 8 polymer chains and 2000 CO$_2$.

thickeners. In this work, a series of SC-CO$_2$ thickeners were designed and prepared to solve the high cost and high pollution of fluoropolymers and cosolvents. The thickener has excellent solubility, thickening property, heat resistance, and pressure resistance.

A series of SC-CO$_2$ thickeners were designed and prepared by molecular simulation. The chemical structures of the copolymers were characterized by FT-IR, ^{1}H-NMR, and GPC. The solubility of the thickener in SC-CO$_2$ was studied using a visual reactor. The response of the thickener to the apparent viscosity of SC-CO$_2$ under different conditions was studied using a self-designed capillary viscometer. The intermolecular interaction energy, radial distribution function (RDF), and cohesive energy

density (CED) of the polymer were calculated to explain its solubility in SC-CO$_2$.

2. Experimental section

2.1 Synthesis and characterization

The materials used in the experiment were octamethylcyclotetrasiloxane (D4, 98%), 1,1,3,3-tetramethyldisiloxane (TMD, 98%), ethylene glycol dimethacrylate (98%), triethylene glycol dimethacrylate (95%), trimethylolpropane trimethacrylate (98%), and H$_2$Cl$_6$Pt·6H$_2$O (99.99%), which were purchased from Aladdin. H$_2$SO$_4$ (98%) was purchased from Sinopharm Chemical Reagent Co., Ltd. Ethylene glycol dimethacrylate, triethylene glycol dimethacrylate, and trimethylolpropane trimethacrylate were washed three times with a 3% NaOH alkali solution to remove MEHQ (p-hydroxyanisole) and then washed three times to remove NaOH. Anhydrous magnesium sulfate was dried, filtered to remove magnesium sulfate, distilled to remove residual alkali, and then refrigerated at low temperatures.

First, add 1 g TMD and 50 g D4 to the hydrothermal reactor, and use 3–4 drops of sulfuric acid (90 °C, N$_2$ atmosphere) as a catalyst to prepare the crude product of Si–H terminal chain siloxane by ring-opening polymerization.[18] Then, sodium carbonate was added to the crude product to remove the catalyst, and the impurities were removed by vacuum distillation to obtain pure Si–H-terminated polysiloxane. In the third step, 4 g of ethylene glycol dimethacrylate was added to a 250 mL three-necked flask equipped with a thermometer, condenser, and magnetic stirring device, 40 ppm chloroplatinic acid was activated at 70 °C for 2 h, and hydrosilylation[19] was reacted for 4 h. To remove chloroplatinic acid, 1 g activated carbon was added to the product, the hydrosilylation reaction was stopped, and the mixture was repeatedly washed with distilled water. Under the vacuum conditions of 370 K and 0.06 MPa, small-molecule compounds and water were removed using a rotating evaporator, and the final product HS-1 was obtained. The Si–H-terminated polysiloxane was reacted with unsaturated
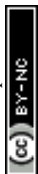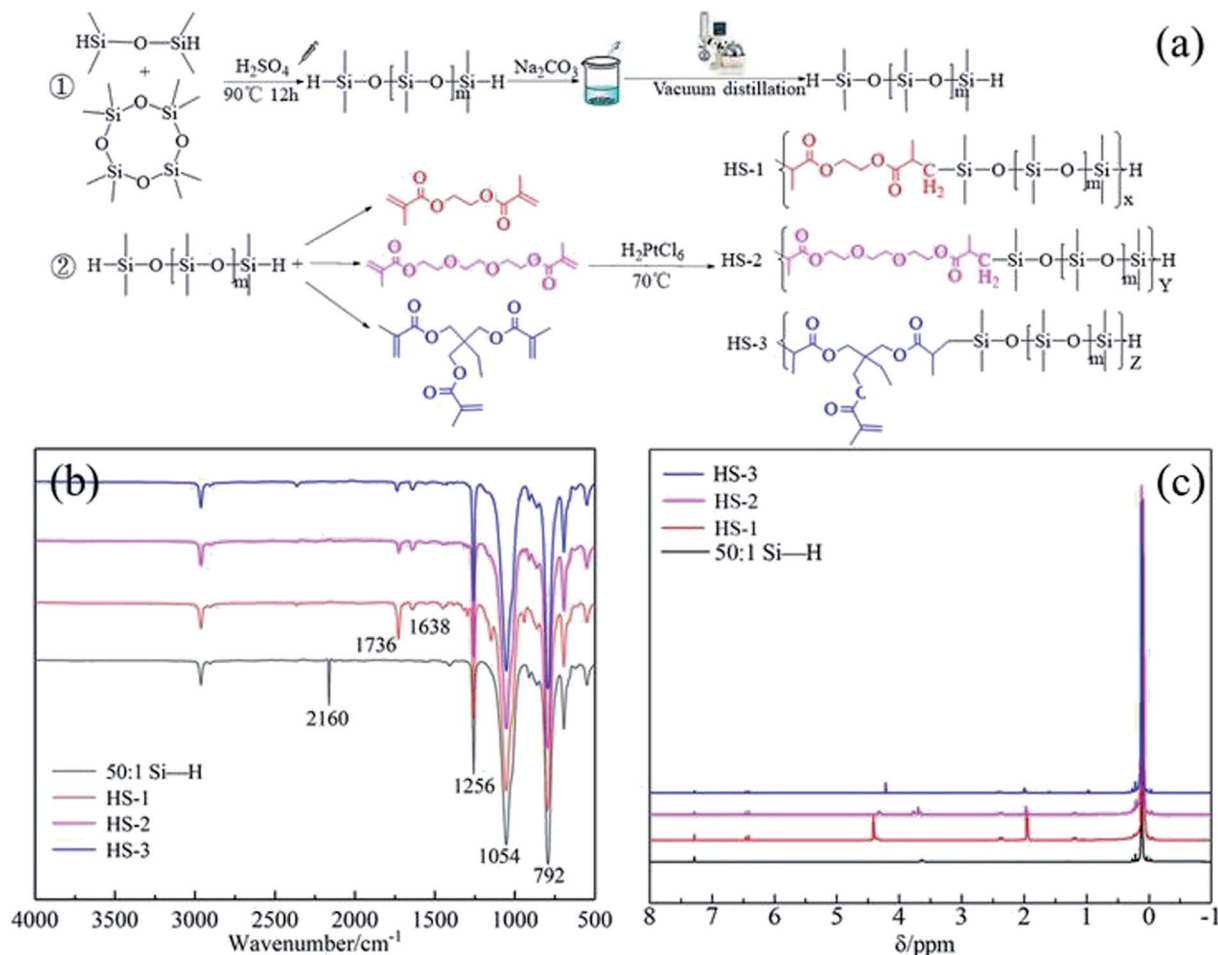
Fig. 4 (a) Synthetic route of HS series thickener (b) Infrared spectrum of HS series thickener(c)HS series thickener hydrogen NMR spectrum.

acrylate, in turn, to obtain thickeners HS-2 and HS-3. The synthetic route is shown in Fig. 4a.

2.1.1 FI-IR measurements. The polymer was characterized by FT-IR using a Nicolet IS50 instrument. After washing the ATR (attenuated total reflection) crystal with ethanol, 0.10 mL of the sample was spread evenly on the surface of the ATR. The scan number of the spectrum is 128 and the resolution is 8 cm^{-1}. The wavenumber ranges from 4000 to 500 cm^{-1}.[20]

2.1.2 ^{1}H NMR measurements. A Bruker-400 MHz NMR was used to record the ^{1}H NMR spectrum[21–23] of the polymer with deuterated chloroform as a solvent.

2.1.3 GPC measurements. The measurement of the polymer molecular weight was completed using a WATERS 2414 refractive index detector. First, 5 mg mL^{-1} polymer solution of chromatographic grade tetrahydrofuran was prepared, and then, the solution was passed to the gel chromatography column at a flow rate of 1 mL min^{-1} at 35 °C.[24]

2.1.4 Cloud point and viscosity measurement. Fig. 2a shows the cloud point measuring device. First, 1 wt% HS thickener (305.15 K) was added to the visualization reactor, switches (1) and (4) were turned on, and a vacuum pump was used to empty the visualization container (the switches not mentioned in each step were closed), and the right side of the

middle container II was filled with water. Second, switches (2), (5), and (6) were turned on, an advection pump was used to compress CO_2 into the liquid in the intermediate container I, switches (2), (4), and (6) were turned on, liquid CO_2 was transferred to the visible container and this was repeated several times until the container was full (every time compress 5 MPa CO_2 gas once and fill up the 500 mL visualization container with (4)–(5) operations). (3) After the thickener and CO_2 were mixed evenly, switches (3), (4), and (6) were turned on, the homogeneous liquid in the visible container was slowly pumped out by a hand pump, and the cloud point phenomenon was observed (pressure when the homogeneous solution is turbid). Throughout the experiment, the advection pump controlled the pressure increase and the manual pump controlled the pressure reduction.

The capillary viscometer (Fig. 2b) consisted of an advection pump, intermediate containers, a differential pressure sensor, and a back-pressure system. In the beginning, the heating area was opened to make the system reach 305.15 K, CO_2 gas entered the intermediate container I containing the thickener under the action of the pump, and CO_2 was repeatedly injected and pressurized until thickened CO_2 reached the supercritical state[25] ($T > 304.25$ K, $P > 7.38$ MPa). Then, the experiment was

Table 1 Chemical shift of siloxane and HS series thickeners

| Polymer category	δ/ppm	Types of H
50 : 1 Si–H terminated polysiloxane	0.17	Si–CH$_3$
	3.60	Si–H
	7.28	CDCl$_3$
HS-1	0.16	Si–CH$_3$
	1.17	O=C–CH(CH$_3$)–CH$_2$
	2.04	CH$_2$=C(CH$_3$)–C=O
	2.6	O=C–CH(CH$_3$)–CH$_2$
	4.41	O–CH$_2$–CH$_2$–O
	6.48–6.50	CH$_2$=C(CH$_3$)–C=O
	7.26	CDCl$_3$
HS-2	0.15	Si–CH$_3$
	1.09–1.18	O=C–CH(CH$_3$)–CH$_2$
	2.01	CH$_2$=C(CH$_3$)–C=O
	2.4	O=C–CH(CH$_3$)–CH$_2$
	3.6–3.8	CH$_2$–O–CH$_2$–CH$_2$–O–CH$_2$
	4.38	O=C–O–CH$_2$
	6.48–6.50	CH$_2$=C(CH$_3$)–C=O
	7.28	CDCl$_3$
HS-3	0.17	Si–CH$_3$
	1.14–1.26	O=C–CH(CH$_3$)–CH$_2$–Si (CH$_2$)$_3$–C–CH$_2$–CH$_3$
	1.60	(CH$_2$)$_3$–C–CH$_2$–CH$_3$
	2.04	CH$_2$=C(CH$_3$)–C=O
	2.4	O=C–CH(CH$_3$)–CH$_2$
	3.8–4.03	(CH$_2$)$_3$–C–CH$_2$–CH$_3$
	6.48–6.50	CH$_2$=C(CH$_3$)–C=O
	7.26	CDCl$_3$
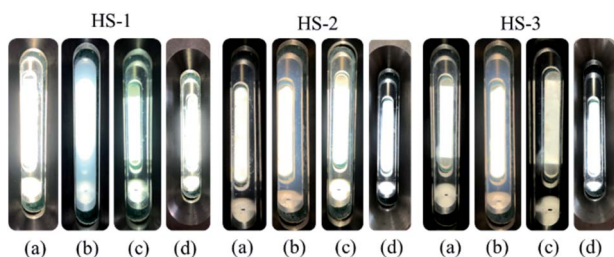
Fig. 5 HS series thickener phase behavior: (a) pure SC-CO$_2$ at 298.15 K, 7.48 MPa; (b) thickener and SC-CO$_2$ mixed phase at 298.15 K, 7.48 MPa; (c) thickener and SC-CO$_2$ mixed phase at 305.15 K, 7.66 MPa; (d) thickener and SC-CO$_2$ mixed phase at 305.15 K, 7.32 MPa.

carried out at a flow rate of 0.18 mL min^{-1} ($\tau = 60$ s^{-1}). The back pressure on the end of the system is 8 MPa. When the system was in equilibrium, the differential pressure in the sensor was recorded and the viscosity was calculated using eqn (1). Eqn (1) is generally suitable for laminar fluids:[26]

$$\eta = \frac{\tau_{\mathrm{w}}}{\gamma_{\mathrm{w}}} = \frac{D\Delta p/4L}{8v/D} \tag{1}$$

where η is the fluid apparent viscosity (Pa s), τ_{w} the wall shear stress (Pa), γ_{w} the apparent shear rate (s^{-1}), D the capillary diameter (m), Δp the pressure difference of capillary (MPa), L the capillary length (m), and v the flow velocity of thickened liquid CO$_2$ (m s^{-1}).

2.2 Materials studio simulation

The polymer simulated in this work was named HS-1, HS-2, and HS-3, and a CO$_2$ system with 2000 CO$_2$ molecules, a polymer system with 8 polymer chains, and a polymer with 8 polymer chains 2000 CO$_2$ molecules were established using the Material Studio software; the all-atom molecular model of the CO$_2$ system is shown in Fig. 3.

In recent years, molecular simulation technology has been widely used in the research field of CO$_2$ thickeners.[9,27] In this work, three kinds of polymer–CO$_2$ boxes (305.15 K, 10 MPa) were constructed with amorphous cells, and through the optimization of the Forcite model and annealing calculation, the dynamic balance system was obtained. The thermostat and barostat were Andersen and Berendsen, respectively. The running time for all the systems was 400 ps, and the trajectories were saved at 1 ps intervals.[23,28,29]

3. Result and discussion

3.1 Structural characterization of HS series thickeners

The four test samples all contain 1256 cm^{-1} (Si–CH$_3$), 1054 cm^{-1} (Si–O),[30] and 792 cm^{-1} (Si–C),[31] as shown in Fig. 4. After the hydrosilylation reaction, HS-1, HS-2, and HS-3 showed C=C and C=O tensile vibration peaks at 1638 cm^{-1} (ref. 32) and 1736 cm^{-1},[33] which were not in 50 : 1 Si–H-terminated polysiloxane, and the Si–H stretching vibration peak (2160 cm^{-1})[34] vanished.
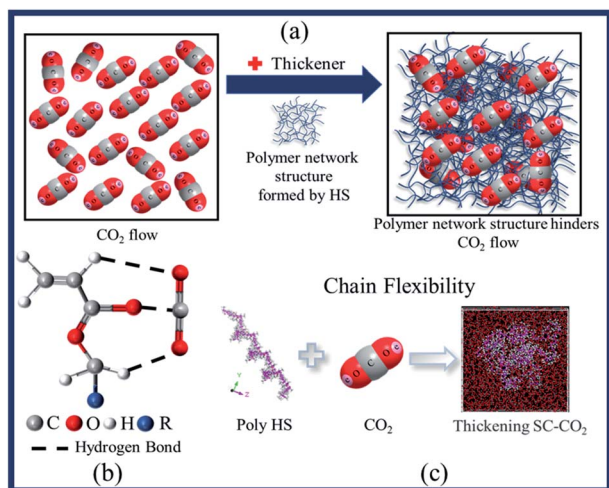
Fig. 6 Dissolution and viscosity-increasing mechanisms of SC-CO$_2$ mainly include (a) polymer–polymer action, (b) polymer–CO$_2$ action, and (c) flexibility polymer of a chain.

The chemical shifts of the four samples shown in Fig. 4 are detailed in Table 1. The results indicate that: (1) the Si–H peaks at 3.6 ppm in 50 : 1 polysiloxane do not appear in HS series thickeners, (2) C=C hydrogen at 6.48–6.50 ppm appears in HS series thickeners. Combining the results of Fig. 5 and Table 1, it was proved that HS series thickeners were successfully prepared.

3.2 Molecular weight analysis

The GPC results of Fig. S1 (ESI†) indicate that the degree of polymerization of 50 : 1 Si–H-terminated polysiloxane is 5, and the molecular weights of HS-1, HS-2, and HS-3 show that the degree of polymerization is 5, 15, and 16, respectively. In a supercritical state, low-content HS-1 may have better solubility, and higher molecular weight HS-2 and HS-3 may have better thickening performance.

3.3 Cloud point

Fig. 5a shows that pure SC-CO$_2$ (298.15 K, 7.48 MPa) in the visualization reactor is transparent. When the visualized reactor
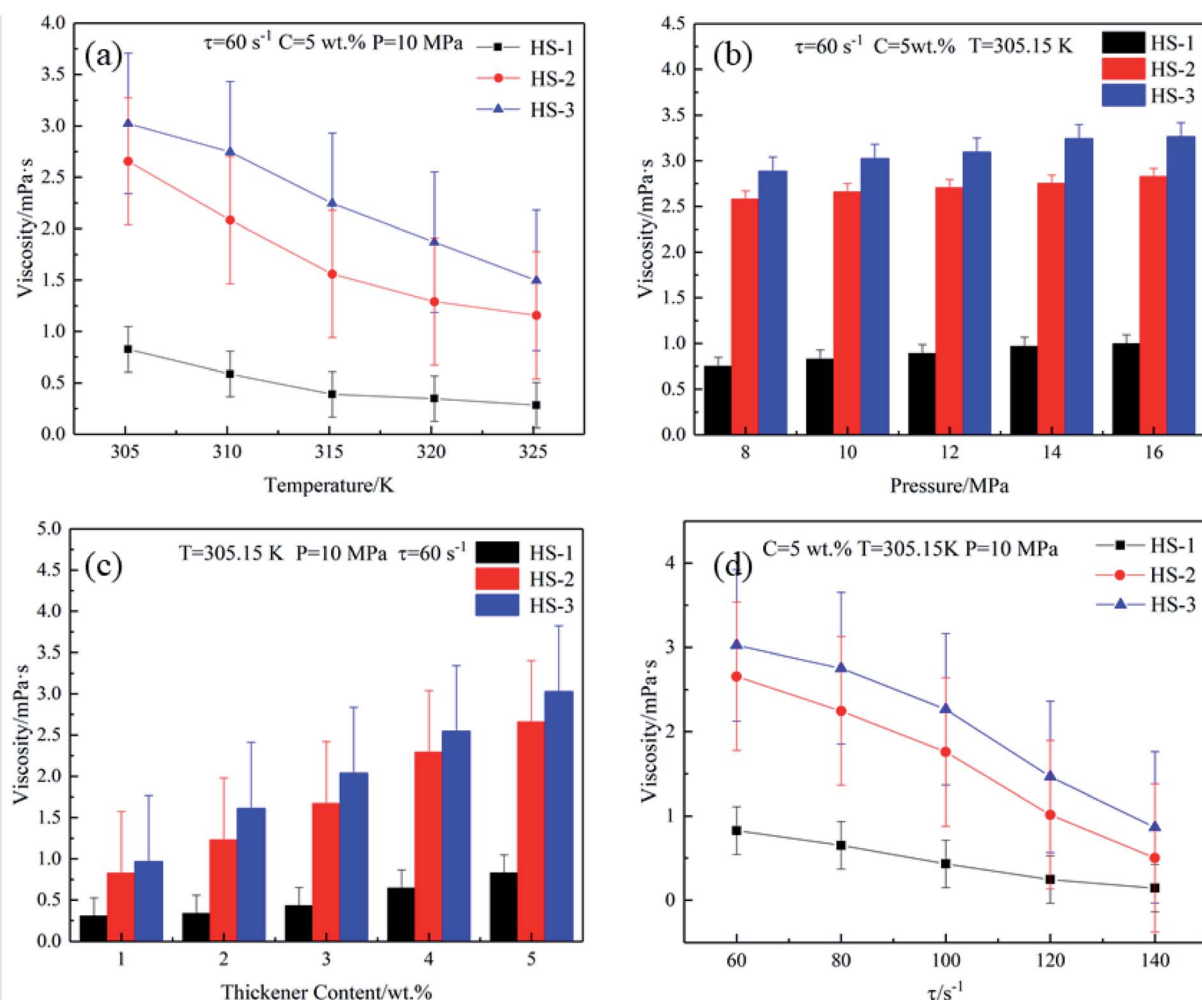

Fig. 7 Effect of different research conditions on apparent viscosity. (a) Influence of temperature on apparent viscosity, (b) influence of pressure on apparent viscosity, (c) influence of thickener content on apparent viscosity, and (d) influence of shear rate on apparent viscosity.
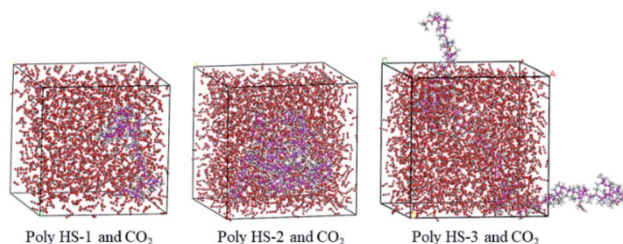
Fig. 8 Dynamic simulation equilibrium conformation of HS series thickeners.

system was composed of HS series thickeners and SC-CO_2, there were two situations: (1) HS-1 was added to SC-CO_2 (298.15 K, 7.48 MPa), and the liquid shows obvious turbidity under white background light and (2) after shaking, SC-CO_2 (298.15 K, 7.48 MPa) was thickened by HS-2, and HS-3 appeared slightly turbid. Finally, the visualization reactor was sealed and placed in a 305.15 K oven to stand for 12 h. After shaking, it can be observed that the three thickened SC-CO_2 (305.15 K, 7.66 MPa) fluids were all in a clear and bright state (Fig. 5c). Fig. 5c and d are the results of the phase behavior study. The instrument in Fig. 2b was used to study the phase behavior (maintaining 305.15 K as a constant temperature condition). According to the experimental results, the three thickening systems remain clear and translucent when the system state reaches the non-critical state of 305.15 K and 7.32 MPa. The HS thickener prepared for this study has no cloud point of supercritical conditions and is a thickener with excellent solubility in SC-CO_2 (no fluoropolymer and co-solvent added).

The introduction to multiple aliphatic groups of the thickener molecule is beneficial for enhancing the solubility. The mechanism is that CO_2 and lipid groups form hydrogen bonds *via* the action of Lewis acids and bases,[35–37] and the good chain flexibility[38,39] of polysiloxane itself also improves the solubility of polymers in SC-CO_2.

3.4 Thickening mechanism and performance

3.4.1 Effect of temperature on the apparent viscosity. The effect of temperature on the apparent viscosity of thickened SC-CO_2 was recorded, as shown in Fig. 7a. In the study range of 305.15–325.15 K, the overall trend was that as the temperature gradually increases, the apparent viscosity of thickened SC-CO_2 gradually decreases. This is consistent with the related research reported in the literature. The reason is that temperature has a certain influence on the network structure formed by polymer chains (Fig. 6a).

The mechanism (Fig. 6a and b) involves the following steps: (1) the HS series polymer chains themselves entangle with each other to form a network structure[40–42] and (2) the hydrogen bond formed by the aliphatic group and CO_2 in the polymerization unit *via* the action of Lewis acid and base further strengthens the network structure.[35–37] When the system temperature increases, the network structure that hinders the flow of CO_2 molecules becomes loose, and the macroscopic performance is that the viscosity decreases. The viscosity of the system will drop sharply until the temperature rises enough to break the hydrogen bond. However, it is worth mentioning that the HS-3 thickener exhibits a certain temperature resistance. This is because there are a certain number of side chains in the polymerization unit, which make the reticular structure formed by the HS-3 thickener more stable than those formed by HS-1 and HS-2.

3.4.2 Effect of pressure on the apparent viscosity. The effect of pressure on the apparent viscosity of thickened SC-CO_2 is depicted in Fig. 7b. Under the conditions where $\tau = 60 \text{ s}^{-1}$, $C = 5$ wt%, and $T = 305.15$ K, the lifting pressure has a positive effect on the viscosity of SC-CO_2 (8–16 MPa). At 16 MPa, the HS-3 thickener has the best thickening effect, reaching 3.26 mPa s.

As explained from the thickening mechanism, the tighter the network structure formed by polymer molecular chains and CO_2 (Fig. 6a), the greater the flow resistance to SC-CO_2, and the macroscopic manifestation shows an increase in apparent viscosity.[42] As the pressure increased, the interaction between the electron-donating groups in the polymer and CO_2 increased, which promoted the increase in apparent viscosity.[43] During the pressurization process, the intermolecular distance gradually decreases, and hydrogen bonds (Fig. 6b) are easier to form.[44] The two effects complement each other and thus have a thickening effect.

3.4.3 Effect of thickener contents on the apparent viscosity. The effect of HS series thickener contents on the apparent viscosity of thickened SC-CO_2 is depicted in Fig. 7c. The research results show that in the concentration range of 1–5 wt% (10 MPa, 305.15 K), the apparent viscosity of the system gradually increases with the increase in the thickener content. At a concentration of 5 wt%, the HS-3 thickener has the best thickening effect, reaching 3.024 mPa s.

The mechanism of action is that with the increase in the thickener content of a closed system, the number of polymer molecular chains that can form a network structure and hydrogen bonds[42] increases multiple times, and the tighter structure greatly hinders the flow of CO_2 molecules. Nevertheless, it takes a lot of energy to destroy the network structure and hydrogen bonds.[45] Under the experimental conditions in this article, there was not enough external energy to destroy the

Table 2 $E_{\text{polymer}-CO_2}$, E_{polymer} and E_{CO_2} parameters of HS series thickeners

System	$E_{\text{polymer}-CO_2}$/kJ mol^{-1}	E_{polymer}/kJ mol^{-1}	E_{CO_2}/kJ mol^{-1}	E_{inter}/kJ mol^{-1}
Poly HS-1 and SC-CO_2	1157.25	−1089.06	1874.10	372.21
Poly HS-2 and SC-CO_2	640.21	−3060.89	1910.25	1790.85
Poly HS-3 and SC-CO_2	791.42	−2784.26	1880.17	1695.51

Table 3 CED and solubility parameter values of the HS series thickeners and CO_2 at 305.25 K and 10 MPa

System	CED/(J m^{-3})	δ/(J cm^{-3})$^{1/2}$	$|\Delta\delta|$/(J cm^{-3})$^{1/2}$
Poly HS-1 and SC-CO_2	1.78×10^8	13.34	0.17
Poly HS-2 and SC-CO_2	1.768×10^8	13.29	0.22
Poly HS-3 and SC-CO_2	1.80×10^8	13.41	0.1
SC-CO_2	1.825×10^8	13.51	0

structure. Therefore, the CO_2 molecules still flowing in the system were captured by the expanding polymer network (Fig. 6a) and macroscopically manifested as an increase in apparent viscosity.

3.4.4 Effect of share rate on the apparent viscosity. Under the conditions where $C = 5$ wt%, $T = 305.15$ K, and $P = 10$ MPa, the increase in shear rate hurts the apparent viscosity of SC-CO_2 (60–140 s^{-1}). It shows that after thickening, SC-CO_2 is a power-law fluid with shear thinning characteristics.[40,46,47] It can be seen from Fig. 7d that the apparent viscosity of HS-1 decreases with the increase in shear rate, which is lower than that of HS-2 and HS-3. The shorter molecular chain of HS-1 is less affected by the increased shear rate. The shorter molecular chain can avoid the shear thinning characteristics, but the short molecular chain often exhibits poor thickening performance. Thickeners HS-2

and HS-3 are more sensitive to the effect of shear rate on apparent viscosity because of longer molecular chains. At 140 s^{-1}, the HS-3 thickener has the best thickening effect, keeping it at 0.86 mPa s.

The HS thickener is a functionalized polysiloxane, which has inherently good chain flexibility (Fig. 6c). With the condition of low shear rate, the shear force is not enough to completely destroy the network structure formed by the entanglement with polymer molecular chains, so that the SC-CO_2 fluid maintains a higher viscosity at a low shear rate. When the shear rate gradually increases, the network structure is gradually destroyed, resulting in a highly oriented arrangement of polymer molecular chains along the shear direction, which reduces the flow resistance of CO_2 (decreases the apparent viscosity).

3.5 Materials studio computational simulation

3.5.1 Dynamic simulation equilibrium conformation. Fig. 8 shows the distribution of three kinds of polymer chains (305.15 K, 10 MPa) in SC-CO_2, where the polymer backbone was marked as purple, and the CO_2 molecules were marked with red oxygen atoms and black carbon atoms. From Fig. 8, it can be observed that after Forcite dynamics simulation, the poly HS-1 and poly HS-2 polymer chains were distributed among a curled state in the amorphous box, while the poly HS-3 polymer chains were distributed in a semi-curved state. The CO_2-
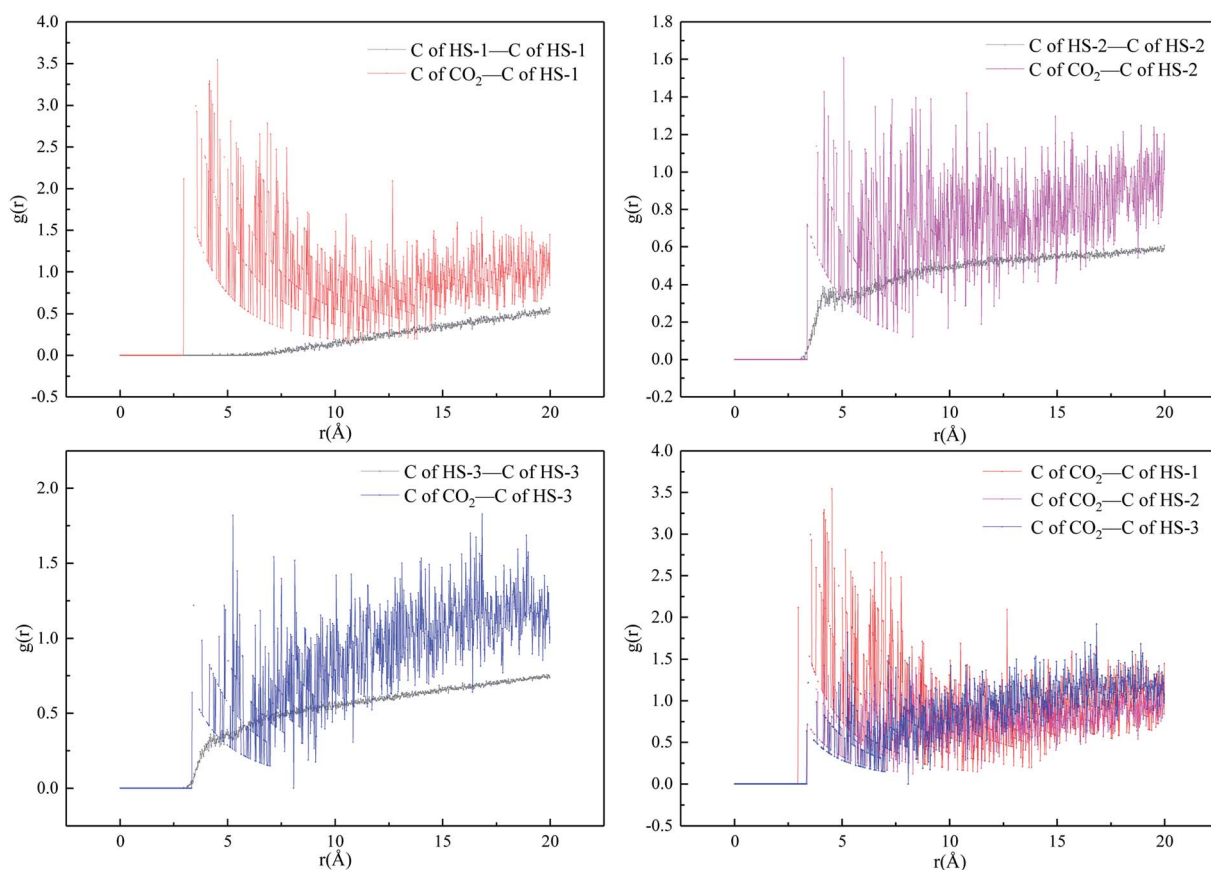
Fig. 9 RDF between HS series thickeners and SC-CO_2.

philic group in poly(HS-1) and poly(HS-2) have a single chain structure, while the branched-chain CO_2 affine monomers in poly(HS-3) increase the richness of the side chains of the polymers. The appropriate amount of side chains makes the polymer chains present wide distribution of simulation results, which was more helpful in the viscosity of SC-CO_2.

3.5.2 Interaction energy calculation. Solving the low viscosity problem of SC-CO_2 depends on the interaction between the polymer and CO_2. The interaction energy (E_{inter}) can be used to measure the strength of this effect. The greater the absolute value of E_{inter} was, the stronger the polymer–CO_2 interaction was. First, the total energy $E_{polymer–CO_2}$ of CO_2–polymer system in a certain frame was calculated. Then, energy E_{CO_2} after removing the polymer chains and energy $E_{polymer}$ after removing the CO_2 molecules were calculated. Finally, interaction energy E_{inter} between CO_2 and polymer chains was obtained using eqn (2) as follows:[48]

$$E_{inter} = E_{polymer–CO_2} - (E_{polymer} + E_{CO_2}) \qquad (2)$$

The $E_{polymer–CO_2}$, $E_{polymer}$ and E_{CO_2} parameters of HS series thickeners are shown in Table 2. From the research data in Table 2, it can be predicted that the solubility of poly HS-2 and poly HS-3 in SC-CO_2 was close and stronger than that of poly HS-1.

3.5.3 Cohesive energy density and solubility parameter calculation. The cohesive energy density (CED) and solubility parameters were used to measure the interaction between polymer molecules. CED is the energy consumed by evaporating 1 mole of polymer per unit volume to overcome intermolecular forces, and the square root of CED was the solubility parameter. The reported research shows that polymers with high solubility in SC-CO_2 usually have lower CED,[38,49,50] and the solubility parameters of polymers and SC-CO_2 are very close.[51] $|\Delta\delta|$ is calculated using formula (3). The CED and solubility parameters (δ) of polymers and SC-CO_2 at 10 MPa and 305.25 K are given in Table 3. According to the results presented in Table 3, HS series thickeners have good solubility in SC-CO_2, and $|\Delta\delta|$ of poly HS-3 and SC-CO_2 was only 0.1 $(J\ cm^{-3})^{1/2}$, indicating that the solubility of HS-3 in SC-CO_2 was the best among the HS series thickeners:

$$|\Delta\delta| = |\delta_{polymer–CO_2} - \delta_{CO_2}| \qquad (3)$$

3.5.4 Radial distribution function calculation. The RDF values between HS series thickeners and SC-CO_2 molecules are represented by the intermolecular RDF of C–C pairs, which are recorded, as shown in Fig. 9. The equilibrium of 400 ps was simulated by force kinetics, and the RDF value of $Inter_{C_{polymer}}$ and $Inter_{C_{polymer}–C_{CO_2}}$ was taken for analysis. If the RDF value of polymer CO_2 is large, it is proved that the HS series thickener is miscible with SC-CO_2.[28,29,48,52,53]

The results shown in Fig. 9 indicate that the RDF values (305.15 K, 10 MPa) of $Inter_{C_{polymer}–C_{CO_2}}$ are generally greater than those of $Inter_{C_{polymer}}$. In the RDF diagram of HS-1, HS-2, HS-3, and CO_2, it can be seen that the three polymers can be dissolved in

SC-CO_2, and the data show a similar trend. Among them, HS-1 showed a larger peak value of the range of 4–7 Å, which was the optimal solution to simulation calculation. This is because the molecular chain of HS-1 was shorter and the molecular weight was lower, resulting in better solubility.

4. Conclusion

In this study, the viscosity of HS series thickeners was studied using a self-designed capillary viscometer. The calculation results indicated that the HS series thickeners have an excellent dissolving effect on SC-CO_2, which provides a new type of feasibility for the design of SC-CO_2 thickeners. At first, polysiloxane had excellent chain flexibility to make HS series thickeners better dispersible in SC-CO_2. Then, the polymer molecular chains were cross-twisted via polymer–polymer interaction to form a spatial network structure, which trapped CO_2 molecules and weakened its fluidity to achieve a thickening effect. Finally, the introduction to multiple lipid groups of the polymerization units of the HS series resulted in (a) excellent solubility and (b) formation of hydrogen bonds between the carbonyl group and CO_2 via Lewis acid–base pairing. It was found that 5 wt% (10 MPa, 305.15 K) HS-3 has the best thickening performance, and the viscosity of SC-CO_2 increases 151 times, reaching 3.024 mPa s. The HS series thickeners prepared for this study can be dissolved in SC-CO_2 without the use of fluoropolymer and co-solvents, which has little damage to the formation and solves the problems of high price and serious pollution by traditional thickeners.

Conflicts of interest

There are no conflicts to declare.

Acknowledgements

References

1 M. Bui, C. S. Adjiman, A. Bardow, E. J. Anthony, A. Boston, S. Brown, P. S. Fennell, S. Fuss, A. Galindo, L. A. Hackett, J. P. Hallett, H. J. Herzog, G. Jackson, J. Kemper, S. Krevor, G. C. Maitland, M. Matuszewski, I. S. Metcalfe, C. Petit, G. Puxty, J. Reimer, D. M. Reiner, E. S. Rubin, S. A. Scott, N. Shah, B. Smit, J. P. M. Trusler, P. Webley, J. Wilcox and N. Mac Dowell, *Energy Environ. Sci.*, 2018, **11**, 1062–1176.

2 V. D. A. Niklas and A. Bardow, *Green Chem.*, 2014, **16**, 3272–3280.

3 N. Mac Dowell, P. S. Fennell, N. Shah and G. C. Maitland, *Nat. Clim. Change*, 2017, 7, 243–249.

4 Z. Dai, H. Viswanathan, R. Middleton, F. Pan, W. Ampomah, C. Yang, W. Jia, T. Xiao, S. Y. Lee and B. McPherson, *Environ. Sci. Technol.*, 2016, **50**, 7546.

5 C. Hepburn, E. Adlen, J. Beddington, E. A. Carter, S. Fuss, N. Mac Dowell, J. C. Minx, P. Smith and C. K. Williams, *Nature*, 2019, **575**, 87–97.

6 M. Godec, *Global technology roadmap for CCS in industry Sectoral Assessment CO2 Enhanced Oil Recovery*, Advanced Resources International[J]. inc., Arlington, VA, 2011, p. 22203.

7 J. Desimone, Z. Guan and C. Elsbernd, *Science*, 1992, **257**, 945.

8 Z. Huang, C. Shi, J. Xu, S. Kilic, R. M. Enick and E. J. Beckman, *Macromolecules*, 2000, **33**, 5437–5442.

9 B. Sun, W. Sun, H. Wang, Y. Li, H. Fan, H. Li and X. Chen, *J. CO2 Util.*, 2018, **28**, 107–116.

10 X. Wang, W. Cheng, Q. Yang, H. Niu and Q. Liu, *J. Environ. Sci.*, 2018, **69**(7), 217–226.

11 M. J. O'Brien, R. J. Perry, M. D. Doherty, J. J. Lee, A. Dhuwe, E. J. Beckman and R. M. Enick, *Energy Fuels*, 2016, **30**, 5990–5998.

12 M. Du, X. Sun, C. Dai, H. Li, T. Wang, Z. Xu, M. Zhao, B. Guan and P. Liu, *J. Pet. Sci. Eng.*, 2018, **166**, 369–374.

13 Q. Li, Y. Wang, Q. Li, G. Foster and C. Lei, *RSC Adv.*, 2018, **8**, 8770–8778.

14 Y. Wang, Q. Li, W. Dong, Q. Li, F. Wang, H. Bai, R. Zhang and A. B. Owusu, *RSC Adv.*, 2018, **8**, 39787–39796.

15 Q. Li, Y. Wang, X. Wang, H. Yu, Q. Li, F. Wang, H. Bai and F. Kobina, *Energy Sources, Part A*, 2019, **41**, 368–377.

16 F. M. Llave, T. H. Chung and T. E. Burchfield, *SPE Reservoir Eng.*, 1990, **5**, 47–51.

17 S. Zhang, Y. She and Y. Gu, *J. Chem. Eng. Data*, 2011, **56**, 1069–1079.

18 J. Chojnowski, *J. Inorg. Organomet. Polym.*, 1991, **1**, 299–323.

19 L. N. Lewis and N. Lewis, *J. Am. Chem. Soc.*, 1986, **108**, 7228–7231.

20 S. Tarhan, *Spectrochim. Acta, Part A*, 2020, **241**, 118714.

21 N. A. Birkin, O. J. Wildig and S. M. Howdle, *Polym. Chem.*, 2013, **4**, 3791–3799.

22 E. Girard, T. Tassaing, L. Catherine, J. D. Marty and M. Destarac, *Macromolecules*, 2012, **45**, 9674–9681.

23 D. Hu, S. Sun, P. Q. Yuan, L. Zhao and T. Liu, *J. Phys. Chem. B*, 2017, **119**, 3194–3204.

24 H. Batzer and S. A. C. Zahir, *J. Appl. Polym. Sci.*, 1975, **19**, 585–600.

25 S. Cummings, D. Xing, R. Enick, S. Rogers, R. Heenan, I. Grillo and J. Eastoe, *Soft Matter*, 2012, **8**, 7044–7055.

26 A. C. Aycaguer, M. Lev-On and A. M. Winer, *Energy Fuels*, 2001, **15**(2), 303–308.

27 A. G. Goicochea and A. Firoozabadi, *J. Phys. Chem. C*, 2019, **123**, 29461–29467.

28 D. Hu, Y. Zhang, M. Su, L. Bao, L. Zhao and T. Liu, *J. Supercrit. Fluids*, 2016, 96–106.

29 D. Hu, S. Sun, P. Q. Yuan, L. Zhao and T. Liu, *J. Phys. Chem. B*, 2015, **119**, 12490–12501.

30 Q. Li, Y. Wang, Q. Li, G. Foster and C. Lei, *RSC Adv.*, 2018, **8**, 8770–8778.

31 B. Altansukh, G. Burmaa, S. Nyamdelger, N. Ariunbolor, A. Shibayama and K. Haga, *Int. J. Soc. Mater. Eng. Resour.*, 2014, **20**, 29–34.

32 A. Svatoš and A. B. Attygalle, *Anal. Chem.*, 1997, **69**(10), 1827–1836.

33 R. Gnanasambandam and A. Proctor, *Food Chem.*, 2000, **68**, 327–332.

34 P. Quintard, G. Ramis, M. Cauchetier, G. Busca and V. Lorenzelli, *J. Mol. Struct.*, 1988, **174**, 369–374.

35 Y. Gu, T. Kar and S. Scheiner, *J. Am. Chem. Soc.*, 1999, **121**, 9411–9422.

36 P. Raveendran and S. L. Wallen, *J. Am. Chem. Soc.*, 2002, **124**, 12590–12599.

37 P. Van Ginderen, W. A. Herrebout and B. J. van der Veken, *J. Phys. Chem. A*, 2003, **107**, 5391–5396.

38 J. DeFelice and J. E. G. Lipson, *Macromolecules*, 2014, **47**, 5643–5654.

39 F. Rindfleisch, T. P. Dinoia and M. A. McHugh, *J. Phys. Chem.*, 1996, **100**, 15581–15587.

40 J. H. Bae and C. A. Irani, *SPE Advanced Technology Series*, 1993, **1**, 166–171.

41 M. D. Doherty, J. J. Lee, A. Dhuwe, M. J. O'Brien, R. J. Perry, E. J. Beckman and R. M. Enick, *Energy Fuels*, 2016, **30**, 5601–5610.

42 X. Luo, S. Wang, Z. Wang, Z. Jing and M. Lv, *J. Pet. Sci. Eng.*, 2015, **133**, 410–420.

43 S. Kilic, S. Michalik, Y. Wang, J. K. Johnson, R. M. Enick and E. J. Beckman, *Ind. Eng. Chem. Res.*, 2005, **42**, 6415–6424.

44 K. Trickett, D. Xing, R. Enick, J. Eastoe and M. J. Hollamby, *Langmuir*, 2010, **26**(1), 83–88.

45 T. Tsukahara, Y. Kayaki, T. Ikariya and Y. Ikeda, *Angew. Chem., Int. Ed.*, 2004, **43**, 3719–3722.

46 T. Tsukahara, Y. Kayaki, T. Ikariya and Y. Ikeda, *Angew. Chem., Int. Ed.*, 2004, **43**, 3719–3722.

47 X. Luo, S. Wang, Z. Wang, Z. Jing, M. Lv, Z. Zhai and T. Han, *J. Pet. Sci. Eng.*, 2015, **133**, 410–420.

48 D. Hu, S. Sun, P. Yuan, L. Zhao and T. Liu, *J. Phys. Chem. B*, 2015, **119**, 3194–3204.

49 Y. Marcus, *J. Supercrit. Fluids*, 2006, **38**, 7–12.

50 P. Raveendran and S. L. Wallen, *J. Am. Chem. Soc.*, 2002, **124**, 7274–7275.

51 H. Lee, J. W. Pack, W. Wang, K. J. Thurecht and S. M. Howdle, *Macromolecules*, 2010, **43**, 2276–2282.

52 P. Gestoso and J. Brisson, *Polymer*, 2003, **44**, 2321–2329.

53 Y. Fu, L. Liao, L. Yang, Y. Lan, L. Mei, Y. Liu and S. Hu, *Mol. Simul.*, 2013, **39**, 415–422.